Toward White Light Emission through Efficient Two-Step Energy Transfer in Hybrid Nanofibers

Varun Vohra,[†,‡,*] Gion Calzaferri,[§] Silvia Destri,[†,‡] Mariacecilia Pasini,[†,‡] William Porzio,[†,‡] and Chiara Botta[†,‡]

[†]Istituto per lo Studio delle Macromolecole (ISMac-CNR), *via* Bassini, 15, Milan 20133, Italy, [‡]Polo Scientifico Tecnologico, CNR, Via Fantoli 16, Milan 20133, Italy, and [§]Department of Chemistry and Biochemistry, University of Bern, Freiestrasse 3, CH-3012 Bern, Switzerland

ABSTRACT Nanosized zeolite L crystals containing about 550 strongly luminescent acceptor molecules have been modified by grafting a conjugated oligomer on their external surface. The 25 nm sized crystals have consequently been embedded in polymeric nanofibers obtained by electrospinning. The fluorescent molecule grafted on the external surface allows addressing the guests in the zeolite nanochannels through an efficient two-step energy transfer from the polymer nanofiber. The so obtained hybrid nanofibers exhibit intense emissions from the three fundamental colors using a single excitation wavelength. The molecule grafted on the external surface of the nanocrystal also induces a higher compatibility of the hybrid organic/inorganic nanomaterials in the conjugated polymer and therefore high concentrations of zeolites embedded in the nanofibers are obtained. Playing on this concentration, the emission of the nanofiber can be tuned and eventually be used for fabricating white-light emitting nanofibers. This hybrid nanomaterial opens new perspectives for low-cost nano organic light emitting diodes fabrication with considerable impact on the lighting and display technologies.

KEYWORDS: zeolite L · nanofibers · FRET · electrospinning · electroluminescent polymer

In the growing world of nanotechnologies, in the past few years, a particular interest has been given to lowering the cost of the electronic materials.[1,2] The idea of using π-conjugated polymers as semiconductors then becomes very appealing.[3] The world of organic electronics is mainly based on conjugated polymers especially when it comes to technologies such as organic light emitting devices (OLED)[4] as well as organic solar cells[5] and organic thin film transistors.[6,7] The idea of using conjugated polymers is widespread even in some commercial applications such as the OLED displays and lighting. Different methods can be used to produce white light from the organic active material.[8,9] The most common consists in using a blend of materials and controlling the energy transfer steps from the material with the higher energy gap to the ones absorbing at lower energies in order to obtain emission from the three fundamental colors (blue, green, and red).[10]

As the technology tends to go toward smaller and smaller scales, obtaining nanoscale objects made of materials with interesting optical and electrical properties is essential.[11] The electrospinning technique is an easy way of obtaining nanofibers of polymeric materials by applying a high voltage between a polymer solution contained in a capillary and a collector counterelectrode.[12−15] The drop formed at the tip of the capillary will stretch due to the electrostatic forces induced by the electric field. This results in the formation of elongated polymeric nanofibers. This technique can be used in different fields going from biomedical[16,17] (*e.g.*, artificial organ components, tissue engineering, wound dressing) to textile, sensors[18] and electronics,[19] photovoltaics[20] and photonics.[21,22]

Some inorganic/organic hybrid materials present major advantages when it comes to increasing the efficiency of the emitting dye and the stability. Zeolite L has been shown to be a successful host material for preparing a large variety of inorganic/organic hybrids.[23] Zeolite L is a crystalline aluminosilicate bearing monodirectional nanochannels created by the hexagonal ionic framework. The channel entrances of zeolite L are of a diameter of 0.71 nm and therefore, by tuning the size and the shape of the organic guest, one can make those guests enter one by one owing to size restrictions. Once in the channels, well-chosen dye molecules stay separated one from another which leads to a higher photoluminescence efficiency as the quenching due to aggregation of the dyes is avoided. Not only does the photoluminescent quantum yield of the dye included in the nanochannels increase but the inorganic crystal also provides a protective framework for the dye inside the nanochannels which will not be

*Address correspondence to varunvohra1984@gmail.com.

Received for review September 3, 2009 and accepted January 27, 2010.

Published online February 4, 2010.
10.1021/nn9017922

subject to photoinduced chemical reactions. The external surface of the zeolite L crystals displays silanol groups that can be further used to functionalize the inorganic host. Such modifications have also been reported for other zeolites, for example, zeolite X.[24] A challenge concerning such host−guest compounds is to be able to optically or electronically address the dye inside the zeolite channels.[25] The hexagonal zeolite crystals bear different surfaces which we can divide into base and coat. The base surfaces have significantly different reactivity compared to the coat surface, partly because the entrance to the main channels is exclusively located at the base surface. This difference forms the bases of the stopcock principle which allows the preparation of very highly organized materials.[23] Using this stopcock approach one can address the dye inside the zeolite channels through a nearly quantitative Förster resonant energy transfer (FRET).[23,26] Energy transfer to a molecule located inside of the nanochannels can also occur from donors located at the coat. It has been shown that for geometrical reasons energy transfer between molecules located at the channel entrances and molecules inside of the channels of zeolite crystals with larger dimensions can in general be expected to be more efficient than between molecules located at the coat and molecules inside of the channels.[25] The difference becomes, however, less important if small crystals in the size range of 100 nm or less are used and if the enhancement of the anisotropy by the stopcock principle is not needed. In this communication, we therefore present results obtained by addressing the dyes inside the zeolite L crystals through an efficient energy transfer from a conjugated organic dye grafted on the total external surface of nanosized crystals. The resulting functionalized zeolite L crystals exhibit an increased miscibility with organic polymers, in agreement with previous reports.[27] The modified zeolite L crystals were embedded in an organic light emitting nanofiber and used as acceptors for FRET. We report a two−step energy transfer process which occurs within the nanofibers and induces photoluminescence of the three fundamental colors as a result of a single wavelength excitation.

RESULTS AND DISCUSSION

The π-conjugated rigid backbone of the organic semiconducting polymers is hardly stretchable and therefore they are not the best materials to be electrospun. A simple way to overcome this problem is to electrospin a blend of the conjugated polymer with a polymer having a flexible backbone.[26,28] The fibers obtained from the electrospinning process were prepared from a blend of a fluorene-based copolymer containing triphenylamine groups (PFTPA) and polyethylene oxide (PEO).

In previous works, PFTPA was shown to avoid formation of fluorenone which quenches the emission from the fluorene inducing a green shift of the emission of the polyfluorene (as can be seen with commercial polyfluorenes).[29,30] Oxonine (Ox^+) loaded zeolites (ZLOx) with α-carboxy-(3,3′′-dihexyl-2,2′:5′,2′′-terthiophene)[31] (T3) or α,ω-dicarbaldehyde-(3,3′′,4′′′,3′′′′′-tetrahexyl-2,2′:5′,2′′,5′′:2′′′:5′′′:2′′′′,5′′′′:2′′′′′-sexithiophene)[32] (T6) grafted on the outer surface were added to the electrospun solution in order to obtain zeolite crystals dispersed in the polymeric nanofiber.

T3ZL and T6ZL respectively correspond to the empty crystals functionalized with T3 and T6. Ox^+-loaded zeolites with T3 or T6 on the external surface will be respectively referred to as T3ZLOx and T6ZLOx. Figure 1 presents the structures of the different molecules that were used along with their optical characterization. The zeolite L anionic framework allows exchange of the counterions with organic cationic dyes. The entrance of the channels is large enough to let one dye molecule such as Ox^+ enter but two molecules cannot pass each other. Therefore, the dye molecules, once inside the channels, do not aggregate and stay separated from each other. The shape and the size of the molecule entering the channels also determines in which way it is oriented with respect to the channel axis. It has been observed that Ox^+ forms an angle of 72° with the channel axis and occupies two repeating units.[33] In this study, 20% of the maximum loading of the zeolite with Ox^+ was found to result in a material in which the nanozeolites are homogeneously filled and where the adsorption on the nanozeolite surface is avoided. It corresponds to a ratio Ox^+ to repeating unit of the zeolite crystals of 1:10 or to a concentration of 0.075 mol/L. Although no aggregation inside the channels occurs, with a higher loading, dishomogeneous dispersion of the dye within the nanochannels (especially close to the channel entrances) appear. In the case of nanozeolites, at a loading of 20% of the maximum loading, such dishomogeneities are not observed.[23]

Nanosized zeolites L of mean diameter and length of 25 nm have been used. One way to graft molecules to their external surface is to first functionalize them with an alkoxysilane derivative.[34] The choice of the alkoxysilane depends on the functions present on the molecule which will be consequently grafted. In the case of T3 and T6, these functions are respectively carboxylic acids or aldehydes. A simple system to link these molecules to the zeolites can be based on the reaction between the acid or the aldehyde and an amine to respectively form an amide and an immine. Therefore, the molecule that was used for the first functionalization step of the surface of the crystals is the aminopropyltriethoxy silane (APTES). The silanol groups present on the external surface (coat and base) of the zeolite react with APTES by forming Si−O−Si bridges. The modified zeolite surface therefore displays amino groups that can be further used for grafting the organic dye. Conse-

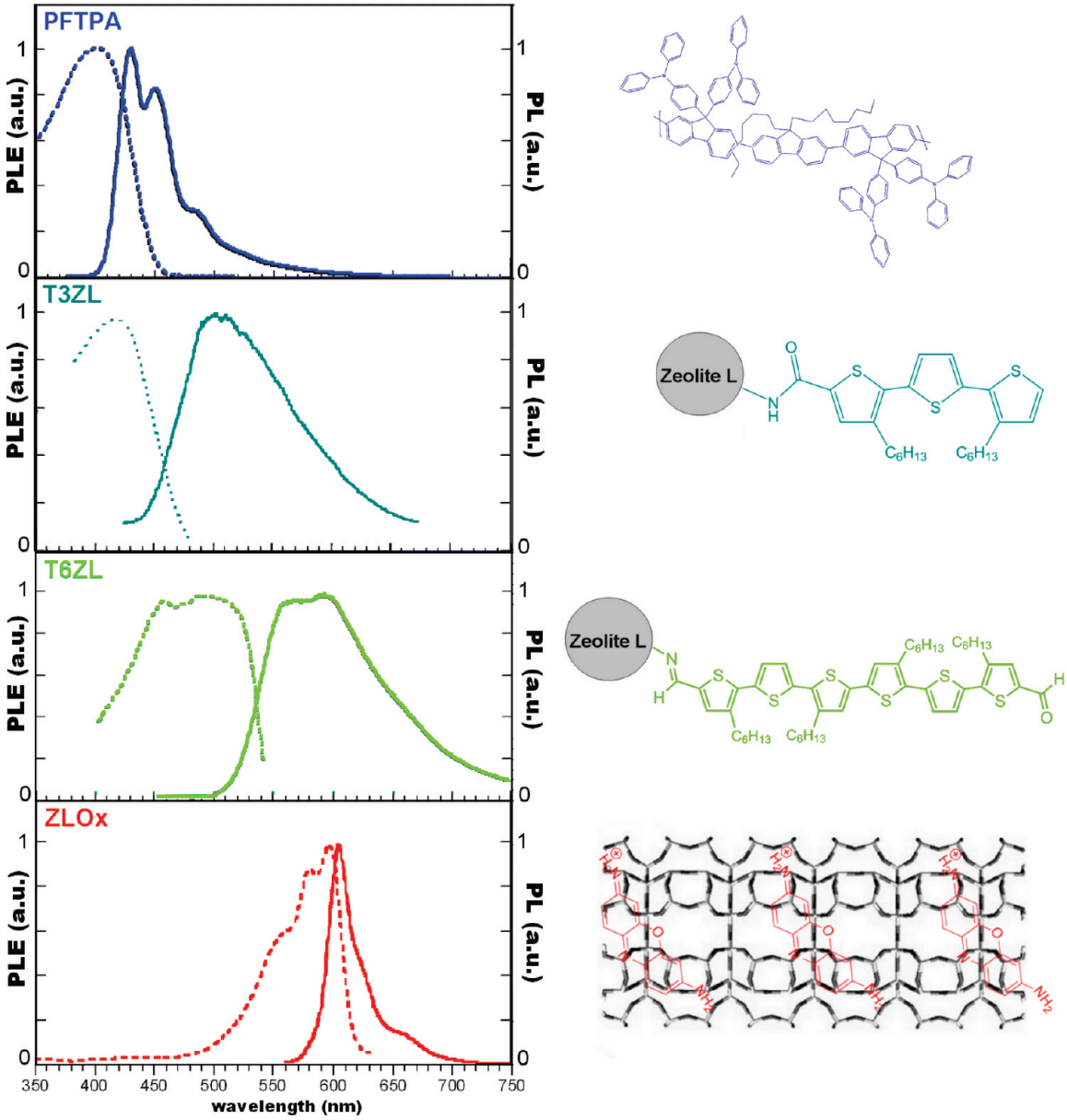

Figure 1. (Dotted line) Photoluminescence excitation profiles (PLE), (solid line) fluorescence spectra (left) and chemical formula (right) of the different molecules composing the system. From top to bottom: PFTPA (film), T3ZL (T3 on zeolite L) powder, T6ZL (T6 on zeolite L) powder, ZLOx (oxonine-loaded zeolite L) powder.

quently T3 or T6 are added to react with the superficial amino groups. T6 was added in large excess (5:1) so that only one of the two aldehyde groups present on T6 reacted with the amino groups. Figure 2 represents the reaction pathway to obtain ZLOx with the grafted T*n*.

To obtain a material which simultaneously emits in three different ranges of wavelengths, it is necessary to have a controlled FRET from the conjugated polymer in the nanofiber to the dye grafted on the zeolite and consequently to the dye inside the channels. Important parameters for FRET are the number of

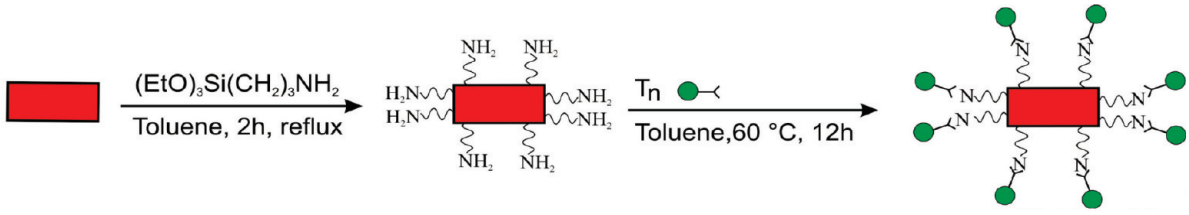

Figure 2. Schematic representation of the functionalization reactions to obtain zeolites with T*n* grafted on the external surface.

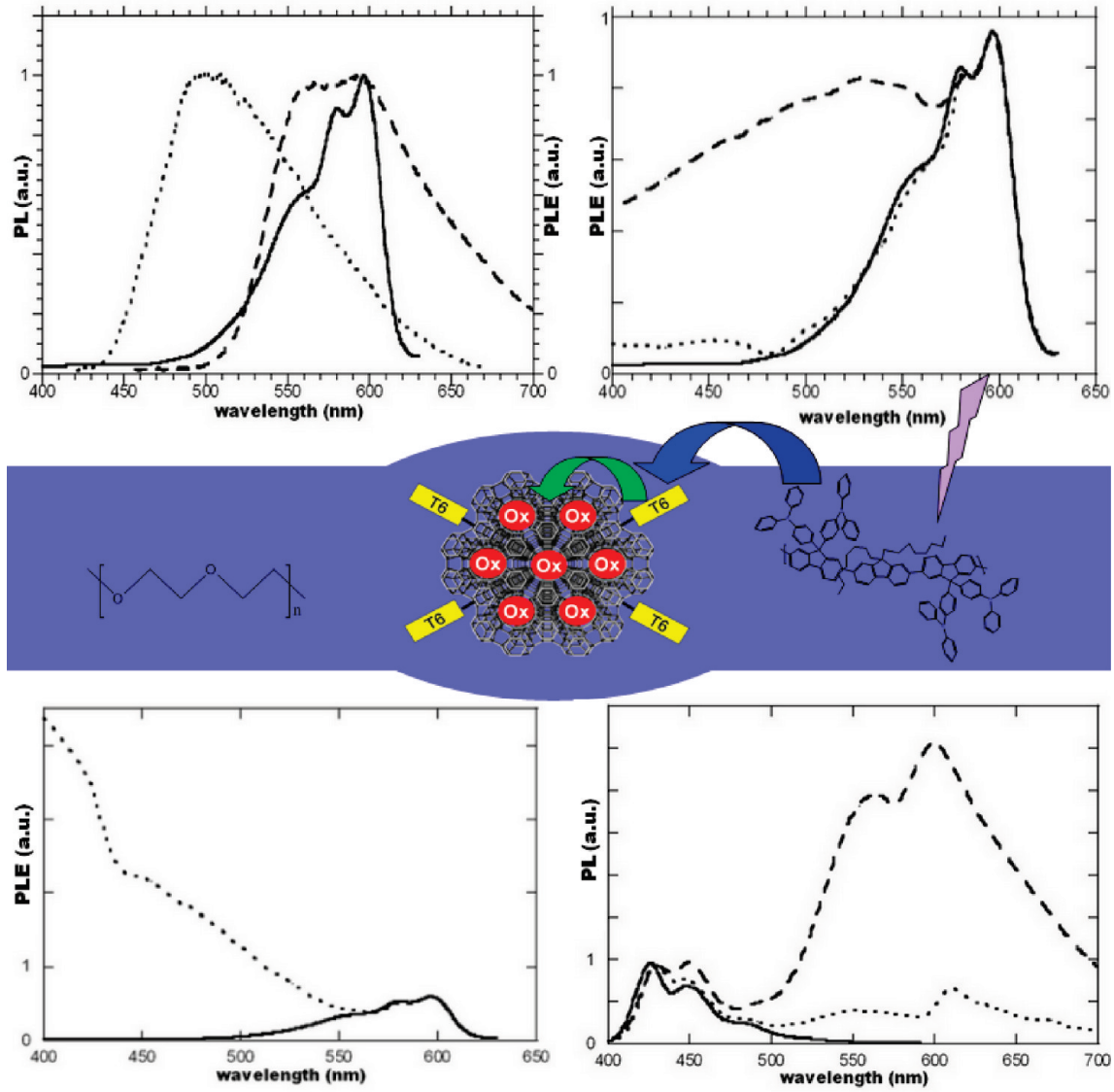

Figure 3. (Top left) PL of T3ZL (dotted line) and T6ZL (dashed line) and excitation profile of ZLOx (solid line); (top right) excitation profiles of ZLOx (solid line), T3ZLOx (dotted line) and T6ZLOx (dashed line); (center) schematic representation of the two-step energy transfer within the fiber; (bottom left) excitation profiles of ZLOx (solid line) T6ZLox dispersed in a PFTPA-PEO blend (dotted line); (bottom right) PL of different concentrations of T6ZLOx dispersed in a PFTPA:PEO blend, wt % = 0 (solid line), 10 (dotted line), and 25 (dashed line). All excitation profiles were integrated between 680 and 700 nm. All PL spectra were obtained with an excitation at 350 nm.

donor−acceptor pairs, as well as the quantum yield of the donor molecule, the molar extinction coefficient of the acceptor, and the spectral overlap between the donor's emission and the acceptor's absorption spectra. The larger the overlap integral is, the more efficient the FRET process becomes.[35] Figure 3 (top left) displays the different overlaps between the photoluminescence of T*n*ZL (the donor) and the excitation profile of ZLOx (the acceptor). As we can see, the overlap between the emission of T6ZL and the excitation profile of ZLOx (which also corresponds to its absorption spectrum) is almost complete, whereas the emission of T3ZL does not overlap very well with the excitation profile of ZLOx. All the excitation profiles displayed in Figure 3 are obtained by integrating the emission between 680 and 700 nm where only the emission from Ox^+ is present. The excitation profiles of ZLOx, T3ZLOX, and T6ZLOx displayed in Figure 3 (top right) confirm that the energy transfer from T6 to Ox+ is very efficient and that, on the other hand, there is almost no FRET from T3 to Ox+. Consequently, we will focus on the system involving T6ZLOx dispersed in a blend of PFTPA:PEO (65:35 in w%) and use the T3ZLOx as a reference in which the two-step energy transfer does not occur. The comparative study of the emission from the blends with T3ZLOx (see Supporting Informations) confirms that Ox+ direct excitation at 350 nm is negligible, which was already introduced in previous works through the Ox+ excitation profiles at higher energies.[23,33]

The comparative study of the excitation profiles of ZLOx alone and T6ZLOx dispersed in the PFTPA:PEO blend (Figure 3, bottom left) demonstrates that a two-step energy transfer from the conjugated polymer to the dye inside the zeolite L crystal is achieved. The system we introduce in this work presents some advantages with respect to the previously introduced zeolite L and stopcock-molecule-based hybrid materials.[26] The first advantage is a huge increase in the experimental FRET efficiency (experimental and theoretical values of respectively 30 and 40%, see experimental section for details) with respect to the previously introduced system.[26] This increase is related mainly to the higher number of donor−acceptor pairs available in this system, which will be the focus of a detailed discussion later.

The second major advantage with respect to the stopcock-molecule-based system is that the compatibility between the T6 present on the surface of the zeolite crystals with polymer materials induces a far better dispersion of the host−guest inclusion compound in the prepared solution and consequently in the polymer film obtained. As can be seen on Figure 3 (bottom right), playing on the concentration of zeolites in the polymer film, the emission can be tuned and we can even obtain white light by combining the emission from PFTPA, T6, and Ox^+. Films containing 10 wt % of T6ZLOx have an emission (recorded with a single excitation at 350 nm) with CIE (Comission Internationale de l'Eclairage) coordinates of (0.33; 0.26).

The calculated values for Förster's radii (R_0) for the systems PFTPA-T6 and T6-Ox+, which correspond to the distances at which the acceptor should be from the donor in order to have a 50% probability for FRET to occur,[35] are respectively 5.7 and 5.0 nm. Such high values for the Förster's radii can be explained by the high overlap between the different donor−acceptor systems, the high photoluminescence quantum yield of the conjugated polymer, and the high molar extinction coefficient of oxonine. (Calculation parameters can be found in the experimental part.) The number of acceptors that are within the reach for FRET by donors grafted at the outer surface of the crystals is determined by the loading of the crystal.

Figure 4 displays the zeolite crystal structure and parameters. Taking into account those geometrical parameters, we can calculate the total number of channels in a 25 nm particle (167 channels) and therefore, the total number of channel openings (334 channel openings). The length of the vector **c** in the zeolite L crystal structure is 0.75 nm. Taking this parameter and the fact that one Ox^+ occupies two unit cells, we find that each 25 nm sized crystal contains 556 Ox^+. As previously observed, it is reasonable to assume that the Ox^+ molecules are homogeneously dispersed in the nanosized zeolite.[23] The calculated Förster's radius for the T6/Ox+ system allows us to calculate the number of Ox+ accessible for energy transfer from molecules

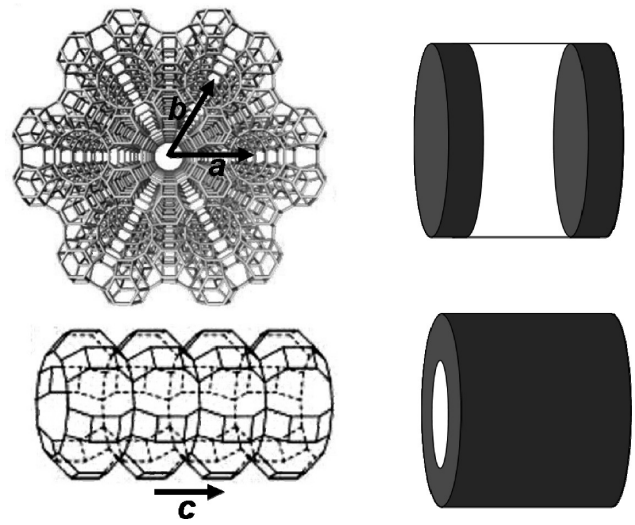

Figure 4. (Left) Crystalline structure of zeolite L; (right) schematic representation of the positions of the Ox^+ which can be excited through energy transfer from the bases (top) and from the coat (bottom) of the zeolite L crystals.

positioned on the different surfaces of the zeolite crystal (base and coat). The number of Ox^+ accessible by T6 attached on the base only is 222 (corresponding to the molecules which stay in the two positions closest to the channel entrances) and the number of Ox^+ accessible by T6 on the coat only is 355 (corresponding to the Ox+ molecules positioned in the two outermost channel rings of the zeolite crystal). Figure 4 (right) gives a schematic representation of the Ox+ molecules within R_0 range for energy transfer from T6 placed either on the base or on the coat. About $^1/_3$ of the acceptors Ox^+ is accessible both from the coat as from the base. From this we find that the total number of Ox^+ within the Förster radius range of donors T6 attached to the whole outer surface is 436. Using both pathways simultaneously, we strongly increase the number of acceptor and donor pairs available for FRET for the nanozised crystals. As a consequence it is easier to meet the conditions for energy transfer from a polymer to the mediator T6 which then transfers to the acceptor inside of the channels than in the system we have recently described.[26]

The electrospinning step will now allow us to obtain nanofibers of a conjugated polymer blended with PEO (Figure 5) embedding T6ZLOx crystals. The confocal images, obtained with a single excitation at 407 nm, exhibit emissions at the different wavelengths corresponding to the polymer, the grafted T6 and the Ox+ molecules. The nanofibers embedding zeolites display mainly blue emission from the polymer but locally exhibit white emission in the parts of the fiber containing zeolites. PL spectra of the nanofibers obtained with different concentrations of zeolite L crystals are analogue to the PL spectra obtained from films of blends with the same concentrations. On Figure 5, we observe that the emission from nanofibers containing different concen-

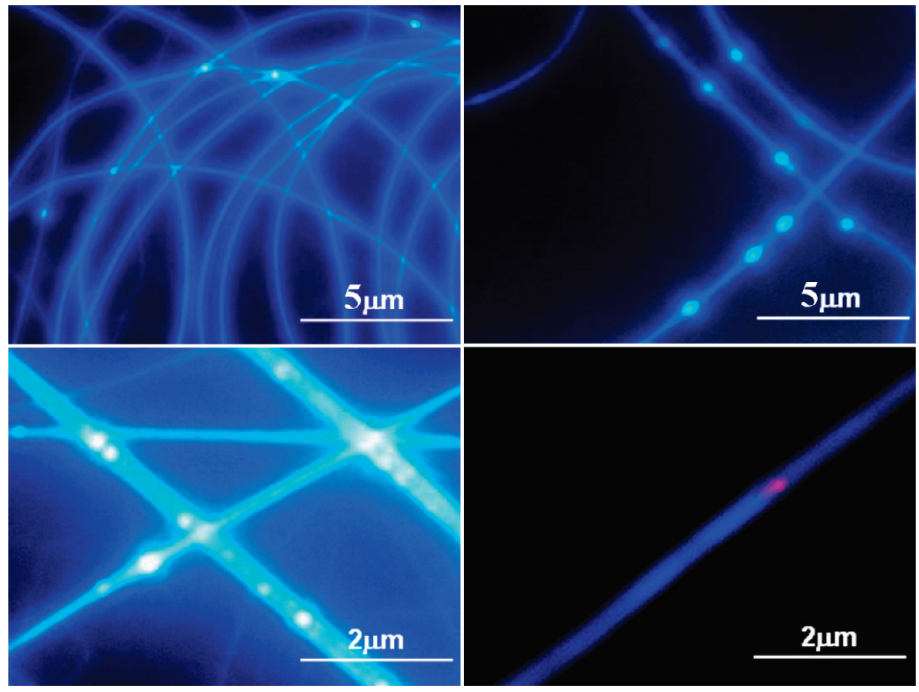

Figure 5. Fluorescence microscope image of fibers of PFTPA-PEO containing 1 wt % (top left), 2 wt % (top right) and 10 wt % (bottom left) of T6ZLOx and confocal microscope image (bottom right) of T6ZLOx in PFTPA-PEO nanofiber .

trations of zeolite crystals can be tuned to obtain white light emitting nanofibers.

CONCLUSIONS

Nanofibers of a blue emitting polymer blend were obtained by electrospinning PFTPA with PEO from toluene. These nanofibers have a mean diameter of 600 nm and display a stable blue emission. We modified dye-loaded nanosized zeolite L crystals' external surface with an appropriate organic molecule which makes them compatible with organic polymers. This compatibility leads to a better dispersion of the zeolite crystals in polymers allowing to increase the amount of zeolite in the polymer and therefore to benefit from the many advantages provided by the zeolite framework on the luminescence properties of the organic dye. Adding such composites to the blend used for electrospinning led to the creation of nanofibers which exhibit a highly efficient two-step FRET to the dye included in the zeolite channels. The conjugated polymer partly transfers its energy to the organic molecule on the surface of the crystals which consequently injects the energy to the final acceptor molecule inside the zeolite channels. This system therefore provides a medium to obtain emission from the zeolite-L-based inclusion compounds, which present many advantages such as the high concentrations which can be obtained avoiding aggregate formation or the protection provided by the zeolite framework against external attacks such as photo-oxidation of the organic dye. The fibers display emissions from the three fundamental colors: blue, green, and red. Playing on the concentrations of the different molecules, electroluminescent white-light emitting hybrid organic/inorganic nanofibers can be created opening perspectives for the fabrication of a new generation of light emitting devices.

METHODS

Preparation of ZLOx. Nano-sized potassium zeolite L, Lucidot, was bought from Clariant.[36] The Ox^+ loading was done as follows. A solution of Ox^+ in water ($c = 1 \times 10^{-4}$ mol · L^{-1}) was prepared. The aimed loading for the samples was 20% of the total loading possible for Ox^+ in the zeolite channels. The required amount of the solution was consequently added to a suspension of zeolites in water, which was then stirred at 80 °C overnight. To collect the loaded zeolites, the suspension was then centrifuged at 5000 rpm for 20 min. Once the solvent was removed, the zeolites were washed twice with 5 mL of distilled water to remove Ox^+ adsorbed on the zeolite's external surface and finally dried in oven at 75 °C.

Preparation of T3ZLOx. T3ZLOx corresponds to ZLOx with T3 grafted all over the external surface of the zeolite crystals. T3 was prepared following the synthetic route presented in literature.[31] Typically 25 mg of Ox^+-zeolite L (10^{-6} moles of −OH groups on the external surface) was suspended in 5 mL of toluene in a polymer tube to which 500 μL (2.14×10^{-3} moles) of APTES (Sigma-Aldrich) was added. The mixture was then sonicated at room temperature for 20 min and stirred for 2 h at 60 °C. To collect the zeolites, the suspension was then centrifuged at 5000 rpm for 20 min. Once the solvent was removed, the zeolites were washed three times with 5 mL of toluene to remove the excess of APTES molecules and finally dried in an oven at 75 °C. The dry zeolites are then resuspended in 10 mL of toluene. Consequently, 1.5×10^{-6} moles of T3 were added to the solution. The mixture was then sonicated at room temperature for 20 min and stirred overnight at 60 °C. The recovery and washing steps were the same as previously; although after the T3 grafting the sample was washed five times in toluene (a good solvent

for T3) instead of two to ensure that all the excess of T3 has been removed completely. The complete removal of unattached T3 was confirmed by fluorescence spectroscopy measurements.

Preparation of T6ZL0x. T6ZLOx corresponds to ZLOx with T6 grafted all over the external surface of the zeolite crystals. T6 was prepared following the synthetic route presented in a previous work.[32] The procedure for grafting T6 to the external surface of the zeolites is similar to the grafting of the T3 presented above. The only difference consists in the fact that T6, unlike T3, was added in excess (5.6×10^{-6} moles or 5 mg). The complete removal of unattached T6 was confirmed by fluorescence spectroscopy measurements.

Preparation of Luminescent Nanofibers. The conjugated polymer used in the fiber is a fluorene-based copolymer containing triphenylamine groups (PFTPA) prepared as described previously,[29,30] blended with PEO bought from Sigma Aldrich. Typically, 20 mg of PFTPA and 10 mg of PEO were added to 1 mL of chloroform and stirred for 10 min at 50 °C in order to avoid phase segregation from the polymers. A relatively large amount of dye-loaded zeolites (typically 3 mg) was added to the blend solution and put in an ultrasonic bath for 20 min. The mixture was then stirred overnight at room temperature in order to disperse the zeolites. The electrospinning apparatus consisted of a high voltage power supply (FC 30R04 Glasmman), a capillary with a diameter between 0.5 and 2 mm containing a platinum-wire electrode and collector-screen counterelectrode placed 5−10 cm from the capillary tip. The potential between the electrodes used for the experiments ranged from 20 to 30 kV.

Optical Characterization of the Different Molecules, Study of the Energy Transfer and Microscopy of the Fibers. Confocal and fluorescence images were collected with a Nikon Eclipse TE2000-U inverted confocal microscope with a long working distance and using a Plan Apo VC objective (magnification 100, N.A. 1.4). The measurements were done with a single excitation wavelength using a DAPI diode laser at 407 nm.

UV−vis transmission spectra were obtained with a Lambda-9 spectrometer. The photoluminescence spectra were recorded by using a 270 M SPEX spectrometer equipped with a N_2-cooled CCD by exciting with a monochromatized Xenon lamp. The spectra were corrected for the instrument response. Fluorescence micrographs were obtained through excitation with a 100-W Hg lamp. The quantum yields of the polymer film and the loaded or functionalized zeolites in powders were obtained using a homemade integration sphere following the procedure reported elsewhere.[37] The energy transfer studies were realized by doing the photoluminescence excitation profiles (PLE) of the different systems. An excitation profile is obtained by integrating the emission of a molecule while sweeping the excitation wavelengths. The integrations are then corrected with respect to the change in intensity of the lamp at the different wavelengths by using a rhodamine B as a reference. Corrected integrations are then plotted with respect to the wavelength of excitation to give rise to the excitation profile. In the case of energy transfer studies to Ox+, the integrated emission range was between 680 and 700 nm. Concerning the other molecules (single molecule characterization), the integrated emission corresponded to the emission from each one of the molecules.

Förster's radius are obtained according to the procedure reported elsewhere[35] with pholuminescence quantum yields of 0.55[31,32] and 0.12 for PFTPA and T6ZL, respectively. Extinction molar coefficients for T6 measured in toluene solution and for oxonine in water are 36455[38] and 84100 $cm^{-1} \cdot M^{-1}$, respectively. The orientation factors κ^2 chosen for the systems PFTPA/T6 and T6/Ox^+ were respectively, 0.476 and 2/3. For the system PFTPA/T6, we consider the case of a dye dispersed in a polymer, whereas in the case of the system T6/Ox^+ we use the value of κ^2 for randomly oriented dipole moments. The refractive indices (n) used for the systems PFTPA/T6 and T6/Ox+, respectively, correspond to the index of the polymer and the index of the zeolite which in the present case are both 1.3.

FRET efficiency is described as the photoluminescence intensity of the acceptor over the total photoluminescence intensity of the donor and acceptor.[35] To have an accurate calculation, we have to take into account direct excitation of the acceptor at the excitation wavelength. The emission from the films prepared by dispersing T3ZLOx in the PFTPA:PEO blend in the same conditions (concentration of zeolites in the films, concentration of Ox+ in zeolites) as the studied system (T6ZLOx in PFTPA:PEO) do not display any emission from Ox+ when excited at 350 nm for different zeolite concentrations (see Supporting Information) which confirms what can be observed on the excitation profiles of Ox+ in previous works.[23,33] We can therefore consider that the direct excitation of Ox+ is negligible with respect to the excitation obtained through energy transfer from T6. The photoluminescence spectra presented in Figure 3 (bottom right) were separated as functions of the three molecules' spectra to obtain the contributions of each one of the molecules. The calculations were made for different samples and the given value is the average of the calculated efficiencies.

Acknowledgment. The work was supported by the European Commission through the Human Potential Program (Marie-Curie RTN 'Nanomatch' Contract No. MRTN-CT-2006-035884; Website: www.nanomatch.eu).

Supporting Information Available: Comparative photoluminescence spectra of PFTPA:PEO blends with and without T3ZLOx. This material is available free of charge *via* the Internet at http://pubs.acs.org.

REFERENCES AND NOTES

1. Ko, S. H.; Pan, H.; Grigoropoulos, C. P.; Luscombe, C. K.; Fréchet, J. M. J.; Poulikakos, D. All Inkjet Printed Flexible Electronics Fabrication on a Polymer Substrate by Low Temperature High Resolution Selective Laser Sintering of Metal Nanoparticles. *Nanotechnology* **2007**, *18*, 345202–345209.
2. Luechinger, N. A.; Athanassiou, E. K.; Stark, W. J. Graphene-Stabilized Copper Nanoparticles as an Air-Stable Substitute for Silver and Gold in Low-Cost Ink-Jet Printable Electronics. *Nanotechnology* **2008**, *19*, 445201–445206.
3. Hines, D. R.; Southard, A.; Fuhrer, S. Poly(3-hexylthiophene) Thin-Film Transistors with Variable Polymer Dielectrics for Transfer-Printed Flexible Electronics. *J. Appl. Phys.* **2008**, *104*, 024510.
4. Burroughes, J. H.; Bradley, D. D. C.; Brown, A. R.; Marks, R. N.; Mackay, K.; Friend, R. H.; Burn, P. L.; Holmes, A. B. Light-Emitting Diodes Based on Conjugated Polymers. *Nature* **1990**, *347*, 539–541.
5. Günes, S.; Neugebauer, H.; Sariciftci, N. S. Conjugated Polymer-Based Organic Solar Cells. *Chem. Rev.* **2007**, *107*, 1324–1338.
6. Murphy, A. R.; Fréchet, J. M. J. Organic Semiconducting Oligomers for Use in Thin Film Transistors. *Chem. Rev.* **2007**, *107*, 1066–1096.
7. Coropceanu, V.; Cornil, J.; da Silva Filho, D. A.; Olivier, Y.; Silbey, R.; Brédas, J.-L. Charge Transport in Organic Semiconductors. *Chem. Rev.* **2007**, *107*, 926–952.
8. Guo, X.; Qin, C.; Cheng, Y.; Xie, Z.; Geng, Y.; Jing, X.; Wang, F.; Wang, L. White Electroluminescence from a Phosphonate-Functionalized Single-Polymer System with Electron-Trapping Effect. *Adv. Mater.* **2009**, *21*, 3682–3688.
9. Lee, P.-I; Hsu, S. L.-C.; Lee, R.-F. White-Light-Emitting Diodes from Single Polymer Systems Based on Polyfluorene Copolymers End-Capped with a Dye. *Polymer* **2007**, *48*, 110–115.
10. Li, Y.; Rizzo, A.; Cingolani, R.; Gigli, G. Bright White-Light-Emitting Device from Ternary Nanocrystal Composites. *Adv. Mater.* **2006**, *18*, 2545–2548.
11. Vohra, V.; Yunus, S.; Attout, A.; Giovanella, U.; Scavia, G.; Tubino, R.; Botta, C.; Bolognesi, A. Bifunctional Microstructured Films and Surfaces Obtained by Soft Lithography from Breath Figure Array. *Soft Matter* **2009**, *5*, 1656–1661.
12. Huang, Z.-M.; Zhang, Y.-Z.; Kotaki, M.; Ramakrishna, S. A Review on Polymer Nanofibers by Electrospinning and Their Applications in Nanocomposites. *Compos. Sci. Technol.* **2003**, *63*, 2223–2253.
13. Sun, Z.; Zussman, E.; Yarin, A. L.; Wendorff, J. H.; Greiner, A.

Compound Core−Shell Polymer Nanofibers by Co-electrospinning. *Adv. Mater.* **2003**, *15*, 1929–1932.
14. Yu, J. H.; Fridrikh, A. V.; Rutledge, G. Production of Submicrometer Diameter Fibers by Two-Fluid Electrospinning. *Adv. Mater.* **2004**, *16*, 1562–1566.
15. Li, D.; Xia, Y. Electrospinning of Nanofibers: Reinventing the Wheel? *Adv. Mater.* **2004**, *16*, 1151–1170.
16. Li, W. J.; Laurencin, C. T.; Caterson, E. J.; Tuan, R. S.; Ko, F. K. Electrospun Nanofibrous Structure: A Novel Scaffold for Tissue Engineering. *J. Biomed. Mater. Res.* **2002**, *60*, 613–621.
17. Hong, Y.; Li, Y.; Zhuang, X.; Chen, X.; Jing, X. Electrospinning of Multicomponent Ultrathin Fibrous Nonwovens for Semi-Occlusive Wound Dressings. *J.Biomed. Mater. Res. A* **2009**, *89*, 345–354.
18. Wang, X.; Kim, Y.-G.; Drew, C.; Ku, B.-C.; Kumar, J.; Samuelson, L. A. Electrostatic Assembly of Conjugated Polymer Thin Layers on Electrospun Nanofibrous Membranes for Biosensors. *Nano Lett.* **2004**, *4*, 331.
19. Pinto, N. J.; Johnson, A. T.; MacDiarmid, A. G.; Mueller, C. H.; Theofylaktos, N.; Robinson, D. C.; Miranda, F. A. Electrospun Polyaniline/Polyethylene Oxide Nanofiber Field-Effect Transistor. *Appl. Phys. Lett.* **2003**, *83*, 4244–4246.
20. Drew, C.; Wang, X. Y.; Senecal, K.; Schreuder-Gibson, H.; He, J. N.; Kumar, J.; Samuelson, L. Electrospun Photovoltaic Cells. *J. Macromol. Sci., Part A: Pure Appl. Chem.* **2002**, *A39*, 1085–1094.
21. Cucchi, I.; Spano, F.; Giovanella, U.; Catellani, M.; Varesano, A.; Calzaferri, G.; Botta, C. Fluorescent Electrospun Nanofibers Embedding Dye-Loaded Zeolite Crystals. *Small* **2006**, *3*, 305–309.
22. Tomczak, N.; Van Hulst, N. F.; Vancso, G. J. Beaded Electrospun Fibers for Photonic Applications. *Macromolecules* **2005**, *38*, 7863–7866.
23. Calzaferri, G; Lutkouskaya, K. Mimicking the Antenna System of Green Plants. *Photochem. Photobiol. Sci.* **2008**, *7*, 879–910.
24. Zhan, B.-Z.; White, M. A.; Lumsden, M. Bonding of Organic Amino, Vinyl, and Acryl Groups to Nanometer-Sized NaX Zeolite Crystal Surfaces. *Langmuir* **2003**, *19*, 4205–4210.
25. Gfeller, N.; Calzaferri, G. Energy Migration in Dye-Loaded Hexagonal Microporous Crystals. *J. Phys. Chem. B* **1997**, *101*, 1396–1408.
26. Vohra, V.; Devaux, A.; Dieu, L.-Q.; Scavia, G.; Catellani, M.; Calzaferri, G.; Botta, C. Energy Transfer in Fluorescent Nanofibers Embedding Dye Loaded Zeolites L Crystals. *Adv. Mater.* **2009**, *21*, 1146–1150.
27. Suárez, S.; Devaux, A.; Bañnuelos, J.; Bossart, O.; Kunzmann, A.; Calzaferri, G. Transparent Zeolite−Polymer Hybrid Materials with Adaptable Properties. *Adv. Funct. Mater* **2007**, *17*, 2298–2306.
28. Campoy-Quiles, M.; Ishii, Y.; Sakai, H.; Murata, H. Highly Polarized Luminescence from Aligned Conjugated Polymer Electrospun Nanofibers. *Appl. Phys. Lett.* **2008**, *92*, 213305.
29. Giovanella, U.; Pasini, M.; Destri, S.; Porzio, W.; Botta, C. Stabilized Blue Emission from Polyfluorene-Based Light-Emitting Diodes: The Role of Triphenylamine. *Synth. Met.* **2008**, *158*, 113–119.
30. Pasini, M.; Giovanella, U.; Betti, P.; Bolognesi, A.; Botta, C.; Destri, S.; Porzio, W.; Vercelli, B.; Zotti, G. The Role of Triphenylamine in the Stabilization of Highly Efficient Polyfluorene-Based OLEDs: A Model Oligomers Study. *Chem. Phys. Chem.* **2009**, *10*, 2143–2149.
31. Jin, J.; Iyoda, T.; Cao, C.; Song, Y.; Jiang, L.; Li, T. J.; Zhu, D. B. Self-Assembly of Uniform Spherical Aggregates of Magnetic Nanoparticles through $\pi-\pi$ Interactions. *Angew. Chem., Int. Ed.* **2001**, *40*, 2135–2138.
32. Olinga, T.; Destri, S.; Porzio, W. Synthesis and Characterization of 3-Hexyl Multisubstituted α,ω-diformyl-α-oligothiophenes ($n = 3, 6, 8$). *Macromol. Chem. Phys.* **1997**, *198*, 1091–1107.
33. Megelski, S.; Lieb, A.; Pauchard, M.; Drechsler, A.; Glaus, S.; Debus, C.; Meixner, A. J.; Calzaferri, G. Orientation of Fluorescent Dyes in the Nano Channels of Zeolite L. *J. Phys. Chem. B* **2001**, *105*, 25–35.
34. Sun, W.; Ji, J.; Shen, J. Rings of Nanoparticle-Decorated Honeycomb-Structured Polymeric Film: The Combination of Pickering Emulsions and Capillary Flow in the Breath Figures Method. *Langmuir* **2008**, *24*, 11338–11341.
35. Lakowicz, J. R. In *Principles of Fluorescence Spectroscopy*; Kluwer Academic: New York, 1999.
36. Clariant. http://www.nano.zeolite.clariant.com/services/zeolite/internet.nsf/04fa7deb65dc84f9c1256a6200552c10/469a3b8327d751b1c125716900411e50!OpenDocument Accessed January 5, 2010.
37. Moreau, J.; Giovanella, U.; Bombenger, J.-P.; Porzio, W.; Vohra, V.; Spadacini, L.; Di Silvestro, G.; Barba, L.; Arrighetti, G.; Destri, S.; *et al*. Highly Emissive Nanostructured Thin Films of Organic Host-Guests for Energy Conversion. *Chem. Phys. Chem.* **2009**, *10*, 647–653.
38. Maas, H.; Calzaferri, G. Trapping Energy from and Injecting Energy into Dye-Zeolite Nano Antenna. *Angew. Chem.* **2002**, *41*, 2284–2288.